ORIGINAL PAPER

Kinetic modelling of the electrochemical mineralization of organic pollutants for wastewater treatment

Agnieszka Kapałka · György Fóti · Christos Comninellis

Abstract The electrochemical mineralization of organic pollutants is a new technology for treatment of dilute wastewater (COD < 5 g L^{-1}). In this method, use of the electrical energy can produce complete oxidation of pollutants on high oxidation power anodes. An ideal anode for this type of treatment is a boron-doped diamond electrode (BDD) characterized by a high reactivity towards oxidation of organics. In the present work kinetic aspects of organic mineralization is discussed. The proposed theoretical kinetic model on boron-doped diamond anodes is in excellent agreement with experimental results. In addition economic aspects of electrochemical organic mineralization are reported.

Keywords Boron-doped diamond electrode · Electrochemical mineralization · Organic pollutants · Wastewater · Kinetic model

1 Introduction

Biological treatment of polluted water is the most economic process and is used for the elimination of "readily biodegradable" organic pollutants present in wastewater. The situation is completely different when the wastewater contains toxic and refractory (resistant to biological treatment) organic pollutants. One interesting possibility is to

A. Kapałka (✉) · G. Fóti · C. Comninellis (✉)
Institute of Chemical Sciences and Engineering, Ecole Polytechnique Fédérale de Lausanne (EPFL), 1015 Lausanne, Switzerland
e-mail: agnieszka.cieciwa@epfl.ch
e-mail: christos.comninellis@epfl.ch

use a coupled process: partial oxidation—biological treatment. The goal is to decrease the toxicity and to increase the biodegradability of the wastewater before biological treatment. However, optimization of this coupled process is complex and usually complete mineralization of the organic pollutants is preferred. The mineralization of these organic pollutants can be achieved by complete oxidation using oxygen at high temperature or strong oxidants combined with UV radiation. Depending on the operating temperature, the type of used oxidant and the concentration of the pollutants in the wastewater, the mineralization can be classified into three main categories:

Incineration: Incineration takes place in the gas phase at high temperature (820 °C–1100 °C). Its main characteristic is direct combustion with excess atmospheric oxygen. The technology is applied mainly for concentrated wastewater with chemical oxygen demand COD > 100 g L^{-1}.

Wet air oxidation process (WAO): Wet air oxidation (WAO) can be defined as the oxidation of organic pollutants in an aqueous medium by means of oxygen from air at elevated temperature (250–300 °C) and high pressure (100–150 bar). Usually Cu^{2+} is used as a catalyst. The efficiency of the mineralization can be higher than 99% and the main by-products formed in the aqueous phase after the treatment are: acetone, methanol, ethanol, pyridine and methanesulfonic acid. The technology is attractive for treatment of wastewater with moderate concentration. The optimal chemical oxygen demand is in the domain: 50 g/L > COD > 15 g L^{-1}.

Oxidation with strong oxidants: The oxidation of organic pollutants with strong oxidants (H_2O_2, O_3) takes place generally at room temperature. In order to increase the efficiency of mineralization, the oxidation takes place in

the presence of catalyst and UV radiation. This technology is interesting for the treatment of dilute wastewater with COD < 5 g L^{-1}.

The electrochemical method for the mineralization of organic pollutants is a new technology and has attracted a great deal of attention. This technology is interesting for the treatment of dilute wastewater (COD < 5 g L^{-1}) and is in competition with the process of chemical oxidation using strong oxidants. The main advantage of this technology is that chemicals are not used. In fact, only electrical energy is consumed for the mineralization of organic pollutants. Besides our contribution in this field [1–11], many other research groups are active in this promising technology [12–24].

The aim of the present work is to elucidate the basic principles of electrochemical mineralization (EM) using some model organic pollutants. The following points will be treated:

– Mechanism of the electrochemical oxygen transfer reaction
– Influence of anode material on the reactivity of electrolytic hydroxyl radicals
– Determination of the current efficiency in the electrochemical oxidation process
– Kinetic model of organic mineralization on BDD anodes
– Intermediates formed during the EM process using BDD
– Electrical energy consumption in the EM process
– Optimization of the EM process using BDD

2 Mechanism of the electrochemical mineralization

In electrochemical mineralization (EM) reactions oxygen is transferred from water to the organic pollutant using electrical energy. This is the so-called electrochemical oxygen transfer reaction (EOTR). A typical example of EOTR is the anodic EM of phenol (Eq. 1).

$$C_6H_5OH + 11H_2O \rightarrow 6CO_2 + 28H^+ + 28e^- \tag{1}$$
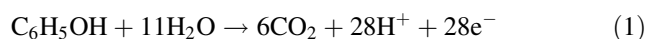
In this reaction water is the source of oxygen atoms for the complete oxidation of phenol to CO_2 at the anode of the electrolytic cell. The liberated protons in this reaction are discharged at the cathode to dihydrogen (Eq. 2).

$$28H^+ + 28e^- \rightarrow 14H_2 \tag{2}$$

According to the generally accepted mechanism of the EM, water is firstly discharged (at potentials above 1.23 V/SHE under standard conditions) at the anode active sites M producing adsorbed hydroxyl radicals (Eq. 3).

$$H_2O + M \rightarrow M(^{\cdot}OH)_{ads} + H^+ + e^- \tag{3}$$
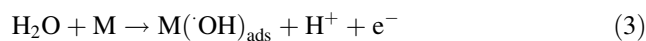
These electrogenerated hydroxyl radicals are involved in the mineralization of organic pollutants R (present in an aqueous solution) (Eq. 4)

$$R_{(aq)} + xM(^{\cdot}OH)_{ads} \rightarrow xM + \text{Mineralization products} + yH^+ + ye^- \tag{4}$$
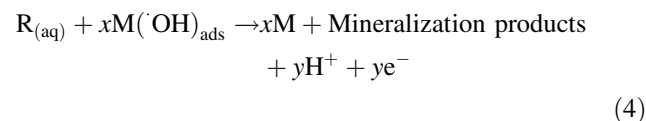
where x and y are the stoichiometric coefficients.

This reaction (Eq. 4) is in competition with the side reaction of the anodic discharge of these radicals to dioxygen (Eq. 5).

$$M(^{\cdot}OH)_{ads} \rightarrow M + \frac{1}{2}O_2 + H^+ + e^- \tag{5}$$
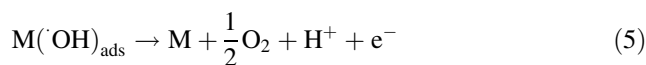
3 Influence of anode material on the reactivity of electrolytic hydroxyl radicals

The reaction of organics with electrogenerated electrolytic hydroxyl radicals (Eq. 4) is in competition with the side reaction of the anodic discharge of these radicals to oxygen (Eq. 5). The activity (rate of reaction 4 and 5) of these electrolytic hydroxyl radicals are strongly linked to their interaction with the electrode surface M. As a general rule, the weaker the interaction, the lower is the electrochemical activity (reaction 5 is slow) toward oxygen evolution (high O_2 overvoltage anodes) and the higher is the chemical reactivity toward organics oxidation. Based on this approach, we can classify different anode materials according to their oxidation power in acid media; this is shown in Table 1. This table shows that the oxidation potential of the anode (which corresponds to the onset potential of oxygen evolution) is directly related to the overpotential for oxygen evolution and to the adsorption enthalpy of hydroxyl radicals on the anode surface i.e. for a given anode material the higher the O_2 overvoltage the higher its oxidation power.

A low oxidation power anode is characterized by a strong electrode-hydroxyl radical interaction resulting in a high electrochemical activity for the oxygen evolution reaction (low overvoltage anode) and to a low chemical reactivity for organic oxidation (low current efficiency for organics oxidation). A typical low oxidation power anode is the IrO_2 based electrode [25]. It has been demonstrated, using differential electrochemical mass spectrometry (DEMS) [26], that the interaction between IrO_2 and hydroxyl radical at this electrode is so strong that a higher oxidation state oxide IrO_3 can be formed. This higher oxide can act as mediator for both organics oxidation and oxygen evolution.
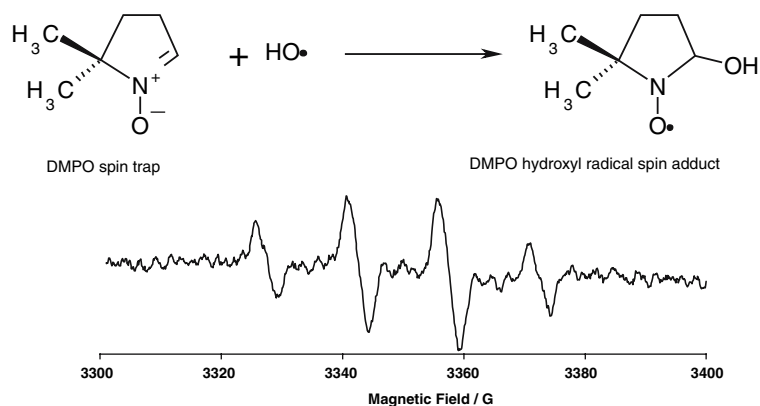
Table 1 Oxidation power of the anode material used in the electrochemical mineralization (EM) process in acid media

Electrode	Oxidation potential / V	Overpotential of O_2 evolution / V	Adsorption enthalpy of M-OH	Oxidation power of the anode
RuO$_2$-TiO$_2$ (DSA-Cl$_2$)	1.4-1.7	0.18	Chemisorption of OH radical	
IrO$_2$-Ta$_2$O$_5$ (DSA-O$_2$)	1.5-1.8	0.25		
Ti/Pt	1.7-1.9	0.3		
Ti/PbO$_2$	1.8-2.0	0.5		
Ti/SnO$_2$-Sb$_2$O$_5$	1.9-2.2	0.7		
p-Si/BDD	2.2-2.6	1.3	Physisorption of OH radical	

In contrast to this low oxidation power anode, the high oxidation power anode is characterized by a week electrode-hydroxyl radical interaction resulting in a low electrochemical activity for the oxygen evolution reaction (high overvoltage anode) and to a high chemical reactivity for organics oxidation (high current efficiency for organic oxidation).

The boron-doped diamond based anode (BDD) is a typical high oxidation power anode [27]. By means of spin-trapping, the formation of hydroxyl radicals on BDD has been demonstrated [28]. The ESR (Electron Spin Resonance) spectrum (Fig. 1) recorded during electrolysis of DMPO (5.5 dimethyl-1-pyrroline-N-oxide) solution on BDD confirms the formation of ˙OH during anodic polarization of diamond electrodes. It has been reported, that the BDD-hydroxyl radical interaction is so weak (no free p or d orbitals on BDD) that the ˙OH can even be considered as quasi free. These quasi free hydroxyl radicals are very reactive and can result in the mineralization of the organic compounds according to Eq. 4. Furthermore, BDD anodes have a high overpotential for the oxygen evolution reaction

compared to platinum (Fig. 2) [29]. This high overpotential for oxygen evolution at BDD electrodes is certainly related to the weak BDD-hydroxyl radical interaction, what results in the formation of H_2O_2 near to the electrode surface (Eq. 6), which is further oxidized at the BDD anode (Eq. 7):

$$2\,^{\cdot}\!OH \rightarrow H_2O_2 \tag{6}$$

$$H_2O_2 \rightarrow 2H^+ + 2e^- + O_2 \tag{7}$$

In fact H_2O_2 has been detected during electrolysis in $HClO_4$ using BDD anodes as shown in Fig. 3 [30].

4 Determination of the current efficiency of the electrochemical mineralization

For the determination of the current efficiency of organic mineralization we consider two parallel reactions:

(a)　The main reaction of oxygen transfer from water toward the organic compound:

$$R + xH_2O \rightarrow \text{Mineralization products} + yH^+ + ye^- \tag{8}$$
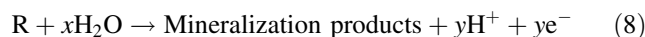
(b)　The side reaction of oxygen evolution:

$$2H_2O \rightarrow O_2 + 4H^+ + 4e^- \tag{9}$$

Two techniques have been proposed for the estimation of the instantaneous current efficiency (ICE) during electrolysis: the chemical oxygen demand (COD) and the oxygen flow rate (OFR) techniques.

4.1 Determination of ICE by the chemical oxygen demand technique

In this technique, the COD of the electrolyte is measured at regular intervals (Δt) during constant current (galvanostatic) electrolysis and the instantaneous current efficiency (ICE_{COD}) is calculated using the relation:
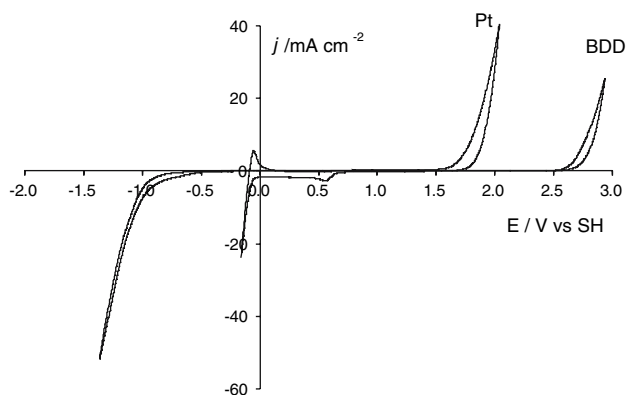
Fig. 1 ESR of DMPO adduct obtained after electrolysis of 8.8 mM DMPO solution in 1 M HClO$_4$ for 2 h on BDD electrode at 0.1 mA cm^{-2}

DMPO spin trap　　　　　　　　　　　　　　　DMPO hydroxyl radical spin adduct

Fig. 2 Cyclic voltammograms of BDD and platinum electrodes; scan rate 50 mVs^{-1} $T = 25$ °C; Electrolyte: 1 M HClO$_4$
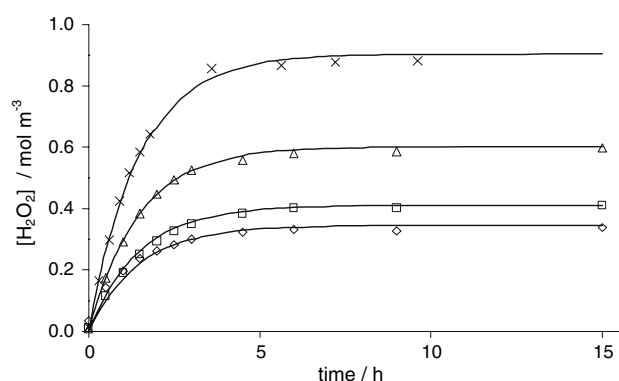

Fig. 3 Production of H$_2$O$_2$ at different current densities; ($\diamond$) 230 A cm^{-2}, ($\square$) 470 A cm^{-2}, ($\triangle$) 950 A cm^{-2}, (x) 1600 A cm^{-2} during electrolysis of 1 M HClO$_4$ on BDD electrode

$$ICE_{COD} = \frac{FV}{8I} \frac{[(COD)_t - (COD)_{t+\Delta t}]}{\Delta t} \qquad (10)$$

where $(COD)_t$ and $(COD)_{t+\Delta t}$ are the chemical oxygen demand (g O$_2$ m^{-3}) at time t and $t + \Delta t$ (s) respectively, I is the applied current (A), F is the Faraday constant (C mol^{-1}) and V is the volume of the electrolyte (m^3).

4.2 Determination of ICE by the oxygen flow rate technique

In the OFR technique the oxygen low rate is measured continuously in the anodic compartment during constant current (galvanostatic) electrolysis in a two compartment electrochemical cell. The instantaneous current efficiency (ICE$_{OFR}$) is then calculated using the relation:

$$ICE_{OFR} = \frac{\dot{V}_o - (\dot{V}_t)_{org}}{\dot{V}_o} \qquad (11)$$

where $\dot{V}_o$(m^{-3} s^{-1}) is the theoretical oxygen flow rate calculated from Faraday's law (or measured in a blank

experiment in the absence of organic compounds) and $(\dot{V}_t)_{org}$(m^{-3} s^{-1}) is the oxygen flow rate obtained during electrochemical treatment of the wastewater.
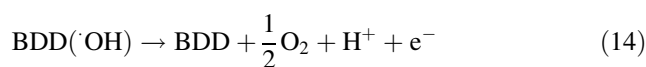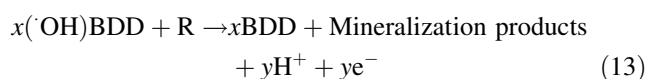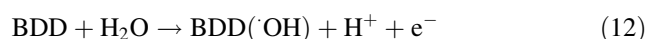
Both the COD and OFR techniques have their limitations as given below:

– If volatile organic compounds (VOC) are present in the waste water only the OFR technique will give reliable results.
– If for example Cl$_2$(g) is evolved during the treatment (due to the oxidation of Cl$^-$ present in the wastewater) only the COD technique will give reliable results.
– If insoluble organic products are formed during the treatment (for example polymeric material) only the OFR technique will give reliable results.

Furthermore, simultaneous application of both the COD and OFR techniques during the electrochemical process will allow better control of the side reactions involved in the electrochemical treatment.

5 Kinetic model of organics mineralization on BDD anode

In this section a kinetic model of electrochemical mineralization of organics (RH) on BDD anodes under the electrolysis regime is presented. In this regime, as reported in the previous section, electrogenerated hydroxyl radicals (Eq. 12) are the intermediates for both the main reaction of organics oxidation (Eq. 13) and the side reaction of oxygen evolution (Eq. 14).

$$BDD + H_2O \rightarrow BDD(\dot{O}H) + H^+ + e^- \qquad (12)$$

$$x(\dot{O}H)BDD + R \rightarrow xBDD + \text{Mineralization products} + yH^+ + ye^- \qquad (13)$$

$$BDD(\dot{O}H) \rightarrow BDD + \frac{1}{2}O_2 + H^+ + e^- \qquad (14)$$

For this simplified reaction scheme (Eqs. 12–14) a kinetic model is proposed based on the following suppositions: (i) adsorption of the organic compounds at the electrode surface is negligible; (ii) all organics have the same diffusion coefficient D; (iii) the global rate of the electrochemical mineralization of organics is a fast reaction and it is controlled by mass transport of organics to the anode surface. The consequence of this last assumption is that the rate of the mineralization reaction is independent of the chemical nature of the organic compound present in the electrolyte. Under these conditions, the limiting current density for the electrochemical mineralization of an organic compound (or a

mixture of organics) under given hydrodynamic conditions can be written as (Eq. 15):

$$i_{\lim} = nFk_mC_{org} \tag{15}$$

where $i_{\lim}$ is the limiting current density for organics mineralization (A m^{-2}), n is the number of electrons involved in organics mineralization reaction, F is the Faraday constant (C mol^{-1}), k_m is the mass transport coefficient (m s^{-1}) and C_{org} is the concentration of organics in solution (mol m^{-3}). For the electrochemical mineralization of a generic organic compound, it is possible to calculate the number of exchanged electrons, from the following electrochemical reaction:

$$C_xH_yO_z + (2x - z)H_2O \rightarrow xCO_2 + (4x + y - 2z)H^+ \\ + (4x + y - 2z)e^- \tag{16}$$
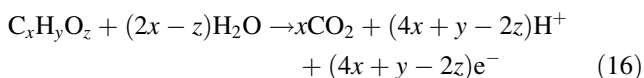
Replacing the value of $n = (4x + y - 2z)$ in Eq. 15 we obtain:

$$i_{\lim} = (4x + y - 2z)Fk_mC_{org} \tag{17}$$

From the equation of the chemical mineralization of the organic compound (Eq. 18),

$$C_xH_yO_z + \left(\frac{4x + y - 2z}{4}\right)O_2 \rightarrow xCO_2 + \frac{y}{2}H_2O \tag{18}$$
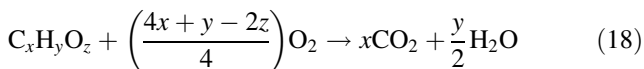
it is possible to obtain the relation between the organics concentration (C_{org} in mol $C_x H_y O_z$ m^{-3}) and the chemical oxygen demand (COD in mol O_2 m^{-3}):

$$C_{org} = \frac{4}{(4x + y - 2z)}COD \tag{19}$$

From Eqs. 17 and 19 and at given time t during electrolysis, we can relate the limiting current density of the electrochemical mineralization of organics with the chemical oxygen demand of the electrolyte (Eq. 20):

$$i_{lim}(t) = 4Fk_mCOD(t) \tag{20}$$

At the beginning of electrolysis, at time $t = 0$, the initial limiting current density ($i_{\lim}^0$) is given by:

$$i_{\lim}^0 = 4Fk_mCOD^0 \tag{21}$$

where COD^0 is the initial chemical oxygen demand.

We define a characteristic parameter α of the electrolysis process (Eq. 22):

$$\alpha = i/i_{\lim}^0 \tag{22}$$

Working under galvanostatic conditions α is constant, and it is possible to identify two different operating regimes: at $\alpha < 1$ the electrolysis is controlled by the applied current, while at $\alpha > 1$ it is controlled by the mass transport control.

(a) Electrolysis under current limited control ($\alpha < 1$).

In this operating regime ($i < i_{\lim}$), the current efficiency is 100% and the rate of COD removal (mol O_2 m^{-2} s^{-1}) is constant and can be written as Eq. 23:

$$r = \alpha \frac{i_{\lim}^0}{4F} \tag{23}$$

Using relation (21), the rate of COD removal (Eq. 23) can be given by:

$$r = \alpha k_m COD^0 \tag{24}$$

It is necessary to consider the mass-balances over the electrochemical cell and the reservoir to describe the temporal evolution of COD in the batch recirculation reactor system given in Fig. 4. Considering that the volume of the electrochemical reactor V_E (m^3) is much smaller than the reservoir volume V_R (m^3), we can obtain from the mass-balance on COD for the electrochemical cell the following relation:

$$QCOD_{out} = QCOD_{in} - \alpha k_m A COD^0 \tag{25}$$

where Q is the flow-rate (m^3 s^{-1}) through the electrochemical cell, COD_{in} and COD_{out} are the chemical oxygen demands (mol O_2 m^{-3}) at the inlet and at the outlet of the electrochemical cell, respectively, and A is the anode
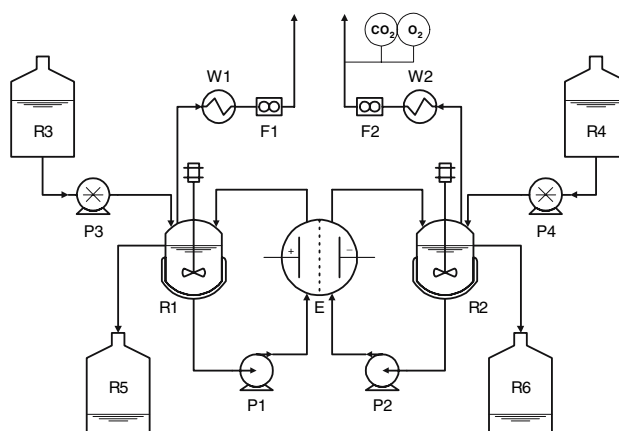

Fig. 4 Scheme of the two-compartments electrochemical flow cell; R—reservoirs; P—pumps; E—electrochemical cell with membrane; W—heat exchangers, F—gas flow controllers; Electrode surface 64 cm^2; Volume of reservoir R1 and R2 250 mL

area (m^2). For the well-mixed reservoir (Fig. 4) the mass balance on COD can be expressed as:

$$Q(COD_{out} - COD_{in}) = V_R \frac{dCOD_{in}}{dt} \qquad (26)$$

Combining Eqs. 25–26 and replacing COD$_{in}$ by the temporal evolution of chemical oxygen demand COD, we obtain:

$$\frac{dCOD}{dt} = -\alpha \frac{COD^0 A k_m}{V_R} \qquad (27)$$

Integrating this equation subject to the initial condition COD = COD^0 at $t = 0$ gives the evolution of COD(t) with time in this operating regime ($i < i_{lim}$):

$$COD(t) = COD^0 \left(1 - \alpha \frac{A k_m}{V_R} t\right) \qquad (28)$$

This behavior persists until a critical time (t_{cr}), at which the applied current density is equal to the limiting current density, which corresponds to:

$$COD_{cr} = \alpha COD^0 \qquad (29)$$

Substituting Eq. 29 in Eq. 28 it is possible to calculate the critical time:

$$t_{cr} = \frac{1-\alpha}{\alpha} \frac{V_R}{A k_m} \qquad (30)$$

or in term of critical specific charge (Ah m^{-3}):

$$Q_{cr} = i_{lim}^0 \frac{(1-\alpha)}{k_m 3600} = \frac{4F COD^0 (1-\alpha)}{3600} \qquad (31)$$

(b)   Electrolysis under mass transport control ($\alpha > 1$).

When the applied current exceeds the limiting one ($i > i_{lim}$), secondary reactions (such as oxygen evolution) commence resulting in a decrease of the instantaneous current efficiency (ICE). In this case, the COD mass balances on the anodic compartment of the electrochemical cell E and the reservoir $R2$ (Fig. 4) can be expressed as:

$$\frac{dCOD}{dt} = -\frac{A k_m COD}{V_R} \qquad (32)$$

Integration of this equation from $t = t_{cr}$ to t, and COD = $\alpha \cdot COD^0$ to COD(t) leads to:

$$COD(t) = \alpha COD \, exp\left(-\frac{A k_m}{V_R} t + \frac{1-\alpha}{\alpha}\right) \qquad (33)$$

The instantaneous current efficiency (ICE) can be defined as:

$$ICE = \frac{i_{lim}}{i} = \frac{COD(t)}{\alpha COD^0} \qquad (34)$$

And from Eqs. 33 and 34, ICE is now given by:

$$ICE = exp\left(-\frac{A k_m}{V_R} t + \frac{1-\alpha}{\alpha}\right) \qquad (35)$$

A graphical representation of the proposed kinetic model is given in Fig. 5. In order to verify the validity of this model, the anodic oxidation of various aromatic compounds in acidic solution has been performed varying organics concentration and current density.

5.1 Influence of the nature of organic pollutants

Figure 6 shows both the experimental and predicted values (continuous line) of both ICE and COD evolution with the specific electrical charge passed during the anodic oxidation of different classes of organic compounds (acetic acid, isopropanol, phenol, 4-chlorophenol, 2-naphtol) [29]. This figure demonstrates that the electrochemical treatment is independent on the chemical nature of the organic compound. Furthermore, there is excellent agreement between the experimental data and predicted values from proposed model.

5.2 Influence of organic concentration

Figure 7 presents both ICE and COD evolution with the specific electrical charge passed during the galvanostatic oxidation (238 A m^{-2}) of 2-naphtol (2–9 mM) in 1 M H$_2$SO$_4$ [31]. As predicted from the model, the critical specific charge Q_{cr} (Eq. 31) increases with increase in initial organic concentration (reported as initial COD^0). Again, there is excellent agreement between the experimental and predicted values.

5.3 Influence of applied current density

The influence of current density on both ICE and COD evolution with the specific electrical charge passed during the galvanostatic oxidation of a 5 mM 2-naphtol in 1 M H$_2$SO$_4$ at different current densities (119–476 A m^{-2}) is shown in Fig. 8 [31]. As previously, excellent agreement between the experimental and predicted values is observed.

a)

$$COD(t) = COD^0\left(1 - \frac{\alpha A k_m}{V_R} t\right)$$

$$COD_{cr} = \frac{i_{appl}}{4F k_m}$$

$$COD(t) = \alpha COD^0 \exp\left(-\frac{A k_m}{V_R} t + \frac{1-\alpha}{\alpha}\right)$$

b) ICE (%)

$$Q_{cr} = i_{cr}^o \frac{(1-\alpha)}{k_m}$$

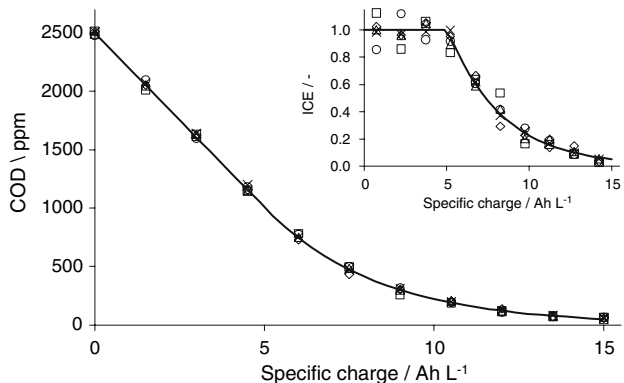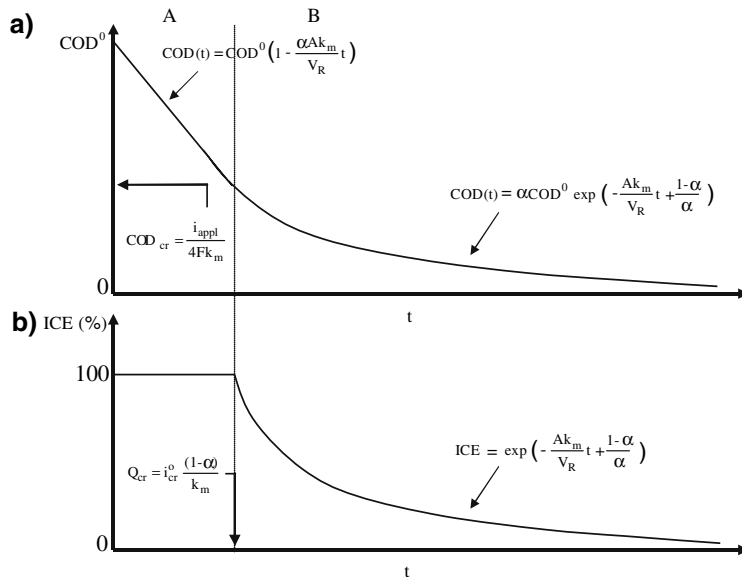$$ICE = \exp\left(-\frac{A k_m}{V_R} t + \frac{1-\alpha}{\alpha}\right)$$

Fig. 6 Evolution of COD and ICE (inset) in function of specific charge for different organic compounds: (x) acetic acid, (□) isopropanol, (o) phenol, (∆) 4-chlorophenol, (◇) 2-naphtol; i = 238 A m^{-2}; T = 25°C; Electrolyte: 1 M H$_2$SO$_4$; The solid line represents model prediction
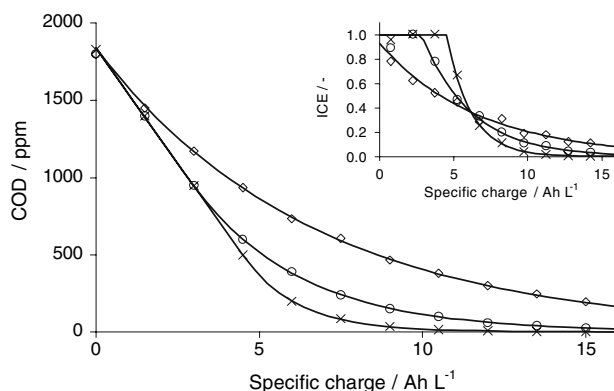

Fig. 8 Influence of the applied current density, (x) 119 A m^{-2}, (o) 238 A m^{-2}, (◇) 476 A m^{-2} on the evolution of COD and ICE (inset) during electrolysis of 5 mM 2-naphtol in 1 M H$_2$SO$_4$ on BDD; T = 25 °C; The solid line represents model prediction
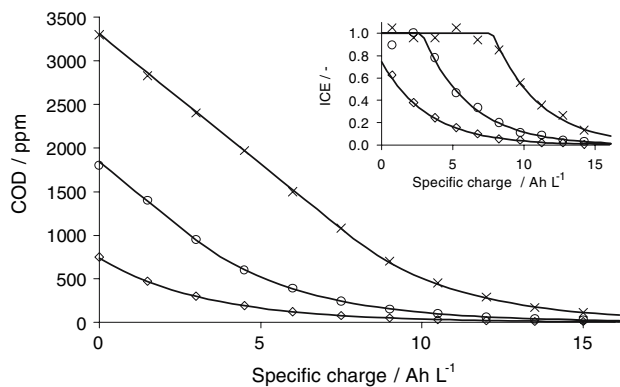

Fig. 7 Influence of the initial 2-naphtol concentration, (x) 9 mM, (o) 5 mM, (◇) 2 mM on the evolution of COD and ICE (inset) during electrolysis on BDD; i = 238 A m^{-2}; T = 25 °C; Electrolyte: 1 M H$_2$SO$_4$; The solid line represents model prediction

6 Intermediates formed during the electrochemical mineralization process

It has been found that the amount and nature of intermediates formed during the electrochemical mineralization of organics on BDD anodes depends strongly on the working regime. In fact, electrolysis under conditions of current limited control results usually in the formation of a significant number of intermediates in contrast to electrolysis under mass transport control, where practically no intermediates are formed and CO$_2$ is the only final product. Figure 9 shows a typical example of phenol oxidation under conditions of current limited control (formation of aromatic intermediates) and mass transport regime (no intermediates, only CO$_2$) [13].
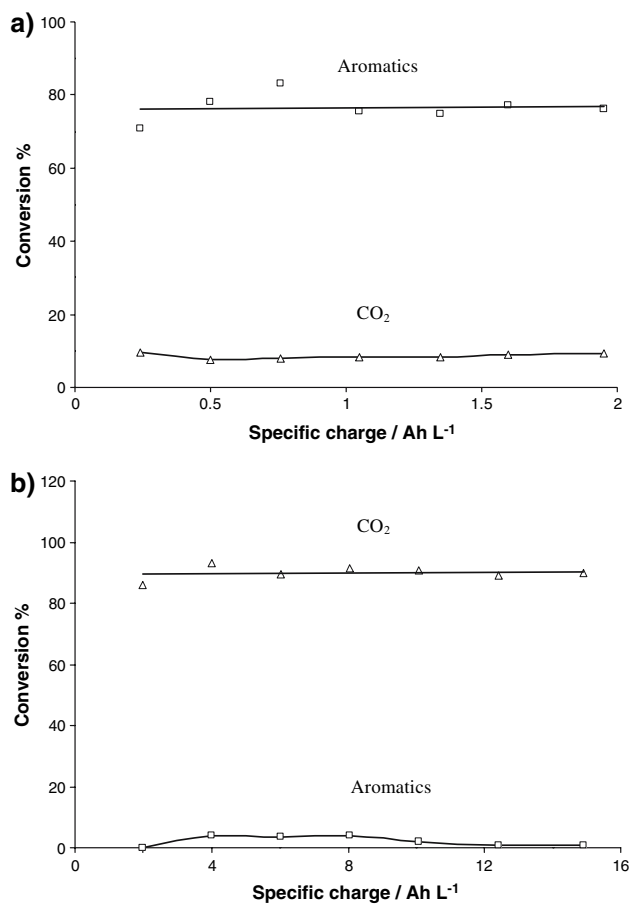
Fig. 9 Trend of the percentage of phenol converted to CO_2 (Δ) and to aromatic compounds ($\square$) during phenol electrolysis in 1 M $HClO_4$ on BDD under (**a**) current limited control, initial phenol concentration: 20 mM, current density 5 mA cm^{-2}; (**b**) mass transport control, initial phenol concentration: 5 mM, current density 60 mA cm^{-2}

7 Electrical energy consumption in the electrochemical mineralization process

In contrast to the chemical oxidation process in which strong oxidants (usually in the presence of catalysts) are used in order to achieve efficient treatment, the electrochemical process consumes mainly electrical energy. The specific energy consumption for the electrochemical treatment of a given wastewater can be estimated from the relation (36) [31]:

$$E_{sp} = \frac{4FV_c}{3600 \text{EOI}} \quad \text{with} \ 0 \leq \text{EOI} \leq 1 \tag{36}$$

where E_{sp} is the specific energy consumption (kWh / kmol COD), F is Faraday's constant (C mol^{-1},) V_c is the cell potential (V) and EOI is the electrochemical oxidation index (which represents the average current efficiency for organics oxidation) given by Eq. 37:

$$\text{EOI} = \frac{\int_0^\tau \text{ICE} dt}{\tau} \quad \text{with} \ 0 \leq \text{EOI} \leq 1 \tag{37}$$

where ICE is the instantaneous current efficiency (–) and τ is the duration of the electrochemical treatment (s). Using the numerical values, Eq. 36 can be written as:

$$E_{sp} = 107.2 \frac{V_c}{\text{EOI}} \quad \text{with} \ 0 \leq \text{EOI} \leq 1 \tag{38}$$

The cell potential can be related to the current density by the relation (Eq. 39):

$$V_c = V_0 + \rho di \tag{39}$$

where V_0 is the constant depending on the nature of the electrolyte (V), ρ is the resistivity of the electrolyte (Ω m), d is the inter-electrode distance (m) and i is the current density (A m^{-2}). Combining Eqs. 38 and 39 gives:

$$E_{sp} = 107.2 \frac{(V_o + \rho di)}{\text{EOI}} \quad \text{with} \ 0 \leq \text{EOI} \leq 1 \tag{40}$$

This relation shows that the specific energy consumption decreases with increasing average current efficiency, reaching a minimum value at EOI = 1.

8 Optimization of the electrochemical mineralization using BDD anodes

As shown in the previous section, the specific energy consumption for the electrochemical mineralization of organics decreases strongly with increasing average current efficiency (EOI) and reaches a minimum value at EOI = 1. In order to work under these favorable conditions (at which EOI = 1), electrolysis has to be carried out under programmed current, in which the current density during electrolysis is adjusted to the limiting value. The following steps are proposed for optimal treatment of a wastewater using BDD anodes:

(a) Measure the initial chemical oxygen demand (COD^0) of the wastewater.
(b) Estimate the mass transfer coefficient (k_m) of the electrolytic cell under fixed hydrodynamic conditions (stirring rate). This can be achieved using a given concentration of Fe(CN)$_6^{4-}$ (50 mM) in a supporting electrolyte (1 M NaCl) and measuring the limiting current (I_{lim}) for the anodic oxidation of Fe(CN)$_6^{4-}$. The mass transfer coefficient (k_m) can then be calculated using the relation:

$$k_m = \frac{I_{\lim}}{FA\left[\text{Fe(CN)}_6^{4-}\right]} \tag{41}$$

where k_m is the mass transfer coefficient (m s^{-1}), I_m is the limiting current (A), $[\text{Fe(CN)}_6^{4-}]$ is the concentration of $[\text{Fe(CN)}_6^{4-}]$ (mol m^{-3}), F is the Faraday constant (C mol^{-1}) and A is the anode surface area (m^2).

(c) Estimate the initial limiting current density ($i_{\lim}$) for the electrochemical mineralization using Eq. 21.

(d) Calculate the time constant of the electrolytic cell (τ_c) using the relation:

$$\tau_c = \frac{V_R}{Ak_m} \tag{42}$$

where τ_c is the electrolytic cell time constant (s), V_R is the volume of the reservoir $R2$ in Fig. 4 (m^3).

(e) Using Eqs. 21, 33, 42 and considering $\alpha = 1$ (initial applied current density = calculated initial limiting current density) we obtain the theoretical temporal evolution of the limiting current during electrolysis (Eq. 42).

$$i_{\lim} = i_{\lim}^0 exp\left(-\frac{t}{\tau_c}\right) \tag{43}$$

(f) Start electrolysis by application of a current density corresponding to the limiting value (calculated as in point c).

(g) Adjust the current density during electrolysis to the time dependent limiting value according to Eq. 43.

(h) From Eqs. 21 and 43, calculate the electrolysis time (τ) in order to achieve the target final COD value (COD$_{final}$) using the relation:

$$\tau = -\tau_c \log \frac{\text{COD}_{final}}{\text{COD}^0} \tag{44}$$

9 Conclusions

This paper summarizes research carried out on electrochemical oxidation of organic pollutants for wastewater treatment over the past 10 years. The nature of the anode material strongly influences the reactivity towards organic oxidation. The key factor in enhanced oxidation is the interaction of electrogenerated hydroxyl radicals with the electrode surface. In general, high oxidation power anodes are characterized by a week electrode-hydroxyl radical interaction resulting in a high current efficiency for organic oxidation and a low electrochemical activity for the oxygen evolution. Based on this, boron-doped diamond can be considered as an ideal anode material for electrochemical mineralization of organic wastes.

The proposed theoretical kinetic model of organic mineralization on boron-doped diamond anodes allows prediction of the evolution of chemical oxygen demand and current efficiency during organic oxidation. The experimental verification of the model at several levels (influence of the nature of the organic pollutants, organic concentration and applied current density) shows excellent agreement with theory in all investigated cases.

References

1. Comninellis Ch, Plattner E (1988) Chimia 42:250
2. Comninellis Ch, Pulgarin C (1991) J Appl Electrochem 21:703
3. Seignez C, Pulgarin C, Peringer P, Comninellis Ch, Plattner E (1992) Swiss Chem 14:25
4. Comninellis Ch (1992) Gas, Wasser, Abwasser 72:792
5. Comninellis Ch, Pulgarin C (1993) J Appl Electrochem 23:108
6. Pulgarin C, Adler N, Peringer P, Comninellis Ch (1994) Water Res 28:887
7. Comninellis Ch (1994) Electrochim Acta 39:1857
8. Comninellis Ch, Nerini A (1995) J Appl Electrochem 25:23
9. Simond O, Schaller V, Comninellis Ch (1997) Electrochim Acta 42:2009
10. Fóti G, Gandini D, Comninellis Ch (1997) Curr Top Electrochem 5:71
11. Ouattara L, Chowdhry MM, Comninellis Ch (2004) New Diam Front Carbon Techn 14:239
12. Comninellis Ch, De Battisti A (1996) J Chim Phys 93:673
13. Iniesta J, Michaud P-A, Panizza M, Cerisola G, Aldaz A, Comninellis Ch (2001) Electrochim Acta 46:3573
14. Chen X, Gao F, Chen G, Yue PL (2003) Environ Sci Technol 37:5021
15. Ouattara L, Duo I, Diaco T, Ivandini A, Honda K, Rao T, Fujishima A, Comninellis, Ch (2003) New Diam Front Carbon Techn 13:97
16. Zanta CLPS, Michaud P-A, Comninellis Ch, De Andrade AR, Boodts JFC (2003) J Appl Electrochem 33:1211
17. Polcaro AM, Mascia M, Palmas S, Vacca A (2004) Electrochim Acta 49:649
18. Brillas E, Boye B, Sires I, Garrido JA, Rodriguez RM, Arias C, Cabot P-L, Comninellis Ch (2004) Electrochim Acta 49:4487
19. Haenni W, Rychen P, Fryda M, Comninellis Ch (2004) Semicond Semimet 77:149
20. Martinez-Huitle CA, Quiroz MA, Comninellis Ch, Ferro S, De Battisti A (2004) Electrochim Acta 50:949
21. Polcaro AM, Vacca A, Mascia M, Palmas S (2005) Electrochim Acta 50:1841
22. Chen X, Gao F, Chen G (2005) J Appl Electrochem 35:185
23. Boye B, Brillas E, Marselli B, Michaud P-A, Comninellis Ch, Farnia G, Sandonà G (2006) Electrochim Acta 51:2872
24. Panizza M, Cerisola G (2005) Electrochim Acta 51:191
25. Fóti G, Gandini D, Comninellis Ch, Perret A, Haenni W (1999) Electrochem Solid-State Lett 2:228
26. Fierro S, Nagel T, Baltruschat H, Comninellis C (2007) Electrochem Commun 9:1969
27. Fóti G, Comninellis C (2004) In: Conway BE, White RE, Vayenas CG (eds) Modern aspects of electrochemistry, vol 37. Kluwer Academic/Plenum Publishers, New York, p 87

28. Marselli B, Garcia-Gomez J, Michaud P-A, Rodrigo MA, Comninellis C (2003) J Electrochem Soc 150:D79

29. Michaud PA (2002) Comportement anodique du diamond synthetique dope au bore, PhD thesis, Ecole Polytechnique Fédérale de Lausanne, Switzerland

30. Michaud P-A, Panizza M, Ouattara L, Diaco T, Foti G, Comninellis C (2003) J Appl Electrochem 33:151

31. Panizza M, Michaud P-A, Cerisola G, Comninellis C (2001) J Electroanal Chem 507:206